Frequency stabilized three mode HeNe laser using nonlinear optical phenomena

Jonathan D. Ellis*, **Ki-Nam Joo, Eric S. Buice, and Jo W. Spronck**

Mechatronic System Design, Delft University of Technology
Mekelweg 2, 2628 CD Delft, The Netherland
j.d.ellis@tudelft.nl

Abstract: Accurate and traceable length metrology is employed by laser frequency stabilization. This paper describes a laser frequency stabilzation technique as a secondary standard with a fractional frequency stability of 5.2×10^{-10} with 2 mW of power, suitable for practical applications. The feedback stabilization is driven by an intrinsic mixed mode signal, caused by nonlinear optical phenomena with adjacent modes. The mixed mode signals are described theoretically and experimentally verified.

OCIS codes: (120.4800) Optical standards and testing; (140.3425) Laser stabilization; (270.3430) Laser theory.

References and links

1. T. J. Quin, "*Mise en Pratique* of the Definition of the Metre (1992)," Metrologia **30**, 523-541 (1994).
2. D. A. Jennings, C. R. Pollack, F. R. Peterson, R. E. Drullinger, K. M. Evenson, J. S. Wells, J. L. Hall, and H. P. Layer, "Direct frequency measurement of the I_2-stabilized He-Ne 473-THz (633-nm) laser," Opt. Lett. **8**, 136-138 (1983).
3. T. H. Yoon, J. Ye, J. L. Hall, and J. -M. Chartier, "Absolute frequency measurement of the iodine-stabilized He-Ne laser at 633 nm," Appl. Phys. B **72**, 221-226 (2001).
4. S. A. Diddams, D. J. Jones, J. Ye, S. T. Cundiff, J. L. Hall, J. K. Ranka, R. S. Windeler, R. Holzwarth, T. Udem, and T. W. Hansch, "Direct link between microwave and optical frequencies with a 300 THz femtosecond laser comb," Phys. Rev. Lett. **84**, 5102-5105 (2000).
5. Th. Udem, R. Holzwarth, and T. W. Hansch, "Optical frequency metrology," Nature **416**, 233-237 (2002).
6. J. Lawall, J. M. Pedulla, and Y. L. Coq, "Ultrastable laser array at 633 nm for real-time dimensional metrology," Rev. Sci. Instrum. **72**, 2879-2888 (2001).
7. F. C. Demarest, "High-resolution, high-speed, low data age uncertainty, heterodyne displacement measuring interferometer electronics," Meas. Sci. Technol. **9**, 1024-1030 (1998).
8. B. A. W. H. Knarren, S. J. A. G. Cosijns, H. Haitjema, and P. H. J. Schellekens, "Validation of a single fibre-fed heterodyne laser interferometer with nanometre uncertainty," Precis. Eng. **29**, 229-236 (2005).
9. T. Baer, F. V. Kowalski, and J. L. Hall, "Frequency stabilization of a 0.633-μm He-Ne longitudinal Zeeman laser," Appl. Opt. **19**, 3173-3177 (1980).
10. R. Balhorn, H. Kunzmann, and F. Lebowsky, "Frequency Stabilization of Internal-Mirror Helium-Neon Lasers," Appl. Opt. **11**, 742-744 (1972)
11. H. S. Suh, T. H. Yoon, M. S. Chung, and O. S. Choi, "Frequency and power stabilization of a three longitudinal mode He-Ne laser using secondary beat frequency" Appl. Phys. Let. **63**, 2027–2029 (1993)
12. S. Yokoyama, T. Araki, and N. Suzuki, "Intermode beat stabilized laser with frequency pulling," Appl. Opt. **33**, 358–363 (1994)
13. J. Y. Yeom and T. H. Yoon, "Three-longitudinal-mode He-Ne laser frequency stabilized at 633 nm by thermal phase locking of the secondary beat frequency" Appl. Opt. **44**, 266–270 (2005)
14. W. E. Lamb, "Theory of an optical maser," Phys. Rev. **134** A1429–A1450 (1964)
15. M. D. Sayers and L. Allen, "Amplitude, competition, self-locking, beat frequency, and time dependent in a three-mode gas laser," Phys. Rev. A **1**, 1730–1746 (1970)
16. H. Dekker, "Theory of self-locking phenomena in the pressure broadened three-mode He-Ne laser," Appl. Phys. **4**, 257–263 (1974)

#121356 - $15.00 USD Received 11 Dec 2009; revised 7 Jan 2010; accepted 11 Jan 2010; published 12 Jan 2010

17. T. Yokoyama, T. Araki, S. Yokoyama, and N. Suzuki, “A subnanometre heterodyne interferometric system with improved phase sensitivity using a three-longitudinal-mode He-Ne laser” Meas. Sci. Technol. **12**, 157–162 (2001)

1. Introduction

Optical frequency standards are widely used in interferometry applications for accurate and traceable length calibration [1]. Iodine absorption spectroscopy is currently the frequency standard for length metrology at 633 nm [1, 2, 3], but recent advances in femtosecond lasers and frequency metrology provide a more stable frequency over a multitude of optical and RF frequencies [4, 5]. These methods are, however, not typically suitable for practical interferometry applications. Instead, secondary standards are employed in a traceable chain and are more suitable in terms of cost, size, and ease of implementation [6].

The motivation for this work is to improve secondary standard lasers for length metrology at 633 nm wavelengths. Higher output power and better frequency stability is needed as more fiber coupling is employed to remote systems and optical paths become longer in precision instruments [7, 8]. Optical frequencies are too fast to detect, thus a signal proportional to the frequency is needed for stabilization. Commonly used methods include Zeeman splitting [9] and two mode intensity balancing [10], both of which have frequency stabilities of 10^{-8} and less than 1 mW of output power. An alternative method uses the secondary beat in a three mode 633 nm Helium Neon laser, which has a fractional frequency stability better than 10^{-10} and higher output power [11, 12, 13].

In this paper, we use a semiclassical model of the three mode laser [14, 15, 16] to describe a frequency stabilization scheme using an intrinsic mixed mode signal. The instrinsic mixed mode signal is directly correlated to the absolute frequency because of nonlinear interactions between adjacent modes. This allows for laser frequency stabilization with a single mode output and high optical power. This research contradicts previous research [11, 12, 13] because the secondary beat frequency, which is akin to the mixed mode signal, cannot be measured without direct measurement of the intermode beat frequencies and subsequent mixing. This is explained theoretically and verified experimentally.

2. Three mode laser model

In previous research, the secondary beat signal, v_b was assumed to be the optical interference between the first and second modes, v_{12}, and the second and third modes, v_{23}, which can be seen in Fig. 1 [11, 12, 13]. A portion of the main beam is split from the laser and a polarizer is used at 45° to interfere the three modes, creating the secondary beat signal, where this signal is detected by a slow speed detector and used for stabilization feedback. The secondary beat frequency, v_b, is on the order of hundreds of kHz, which means direct measurement of the laser’s mode frequency spacing should not be needed.

However, Lamb [14] showed that in addition to the normal main frequencies, i.e., those frequencies whose source is the linear part of the polarization of the active laser medium, there are the so-called combination frequencies whose source is the third-order nonlinear harmonics. The magnitude of the frequency difference between them depends in detail on the exact cavity tuning and the state of excitation of the active medium. Compared to the second-order nonlinear harmonics, it can be always generated without any symmetry restrictions of the medium at the condition of the high intensity such as the HeNe gas inside the laser cavity. Specifically in three mode operation, three additional frequencies, $(2v_2 - v_3)$, $(v_1 + v_3 - v_2)$, and $(2v_2 - v_1)$, are generated near the main frequencies, v_1, v_2 and v_3, respectively. It is noted that besides these three combination frequencies, there are more frequencies which do not produce appreciable effects due to the gain bandwidth and threshold of the medium. In this case, each of the three

#121356 - $15.00 USD Received 11 Dec 2009; revised 7 Jan 2010; accepted 11 Jan 2010; published 12 Jan 2010

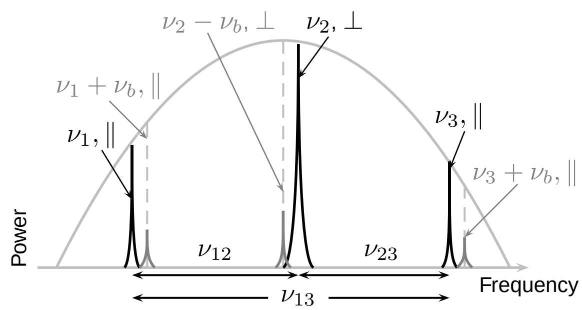

Fig. 1. A schematic of the three laser modes including three additional mixed modes. These modes arise from nonlinear optical interaction between ν_1, ν_2, and ν_3.

main modes are oscillated by the interaction with the adjacent modes, which can be seen in Fig. 1.

These time dependent main frequencies are [16]

$$\nu_1 + \dot{\varphi}_1 = \Omega_1 + \sigma_1 + \rho_1 E_1^2 + \tau_{12} E_2^2 + \tau_{13} E_3^2 - (\eta_{23} \sin\psi - \xi_{23} \cos\psi) E_2^2 E_3 E_1^{-1}, \quad (1)$$

$$\nu_2 + \dot{\varphi}_2 = \Omega_2 + \sigma_2 + \tau_{21} E_1^2 + \rho_2 E_2^2 + \tau_{23} E_3^2 + (\eta_{13} \sin\psi - \xi_{13} \cos\psi) E_1 E_3, \text{ and} \quad (2)$$

$$\nu_3 + \dot{\varphi}_3 = \Omega_3 + \sigma_3 + \tau_{31} E_1^2 + \tau_{32} E_2^2 + \rho_3 E_3^2 - (\eta_{21} \sin\psi - \xi_{21} \cos\psi) E_2^2 E_1 E_3^{-1}, \quad (3)$$

where

$$\psi = (2\nu_2 - \nu_1 - \nu_3)t + (2\varphi_2 - \varphi_1 - \varphi_3) = \nu_b t + \varphi_b \quad (4)$$

and all parameters refer to Lamb's corrected paper [15]. As shown in Eq. (1–3), the main frequencies are time varying with a frequency of ν_b, the same frequency as the secondary beat.

Using the complete model, we assume there are six different modes in the three mode laser, which can be seen in Fig. 1. These include the three main modes (M_i), which are, in the frequency domain,

$$M_1 = \nu_1 + \dot{\varphi}_1 \quad (5)$$

$$M_2 = \nu_2 + \dot{\varphi}_2 \quad (6)$$

$$M_3 = \nu_3 + \dot{\varphi}_3, \quad (7)$$

by removing the time-varying phase function from the adjacent mode and simplifying Eqs. (1–3). The three mixed mode frequencies, which arise from interaction with the adjacent modes, are

$$M_{1,m} = \nu_1 + \nu_b + \dot{\varphi}_b \quad (8)$$

$$M_{2,m} = \nu_2 - \nu_b - \dot{\varphi}_b \quad (9)$$

$$M_{3,m} = \nu_3 + \nu_b + \dot{\varphi}_b, \quad (10)$$

in the absolute frequency domain, where $M_{i,m}$ is the i^{th} mode from lowest to highest frequency and the m idicates a mixed mode. Each mixed mode has the same polarization state as the adjacent main model. This was verified by using a Glan-Thompson polarizer aligned to block the central mode and an optical spectrum analyzer. If the polarization state of the adjacent mixed mode $M_{2,m}$ was different than, M_2, it would be detected by the optical spectrum analyzer (OSA), which was not the case. Additionally, when the outer modes, M_1 and M_3, were blocked, their respective adjacent mixed modes were blocked as well.

#121356 - $15.00 USD Received 11 Dec 2009; revised 7 Jan 2010; accepted 11 Jan 2010; published 12 Jan 2010

3. Experimental verification

To verify the presence of these mixed modes, the experimental setup in Fig. 2 was used. This setup has a common polarizer (p) for all three different detectors, a low speed photodiode (PD, DC–500 kHz), a high speed avalanche photodiode (APD, 1 MHz–1.5 GHz), and an OSA. The low speed detector was used to compare with previous laser stabilization experiments [11, 12, 13]. The avalanche photodiode was use to compare with the previous superheterodyning experiment [17]. The OSA was used to verify the presence each particular mode during an experiment.

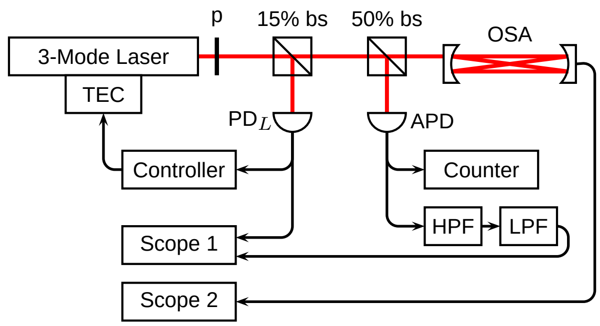

Fig. 2. (Color Online) Optical schematic for characterizing the three mode laser behavior. A common polarizer is used between the three different detectors and a HPF-LPF behaves like a self mixing circuit.

For these experiments, the polarizer was rotated in increments of 15°, starting at 0°, where the central mode (M_2) was only visible on the OSA. From our previous experiments with the three mode laser (25-LHR-121, Melles Griot), the frequency of the secondary beat signal was known to be between 200 and 400 kHz. When a signal in that frequency range was detected on Scope 1, the peak-to-peak value of PD$_L$ and APD was recorded, as shown in Fig. 3. It should be noted, the bandpass filter from the high pass filter (HPF) and low pass filter (LPF) behaves similarly to a self mixing circuit, which was used in research by Yokoyama, *et. al.*[17].

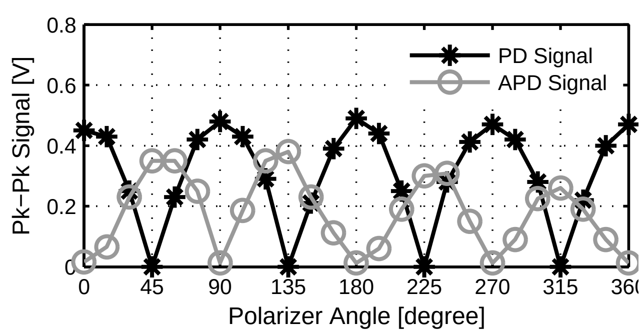

Fig. 3. Measured frequency from both detectors as a function of polarization rotation. The signals are 45° out of phase, which was unexpected.

From these measurements, it is clear the signals from the separate detectors are 180° out of phase (45° based on polarizer angle) meaning the two detectors PD and APD do not measure the same thing, which was not expected. Additionally, these measurements directly contrast previous research [11, 12, 13] where a 45° polarizer angle was used to create the secondary

#121356 - $15.00 USD Received 11 Dec 2009; revised 7 Jan 2010; accepted 11 Jan 2010; published 12 Jan 2010

beat signal without direct measurement of the intermode beat frequencies. To fully explain our results from these experiments and why they contradict previous research, the three additional mixed modes in the semiclassical three mode laser model must be used.

4. Discussion

At a polarizer angle of 0°, the four outer modes, M_1, $M_{1,m}$, M_3, and $M_{3,m}$, are all blocked leaving M_2 and $M_{2,m}$. This is clearly visible on the OSA, however, the resolution is not fine enough to see the mixed mode adjacent to M_2. The two central modes M_2 and $M_{2,m}$ interfere creating the detectable time domain signal

$$I^0_{pd} = \cos\left(2\pi\nu_b t + 3\varphi_2 - \varphi_1 - \varphi_3\right), \tag{11}$$

where I is the irradiance, the superscript indicates the polarizer angle, and the subscript indicates the signal is within the detectable bandwidth for a specific detector. The frequency of ν_b is within the detectable bandwidth of PD and not within the bandwidth of APD, thus, PD only measures the mixed modal frequency.

When the polarizer is at 90°, the opposite effect happens. The two central modes are blocked; the four outer modes interfere and are detected. The time domain signals

$$I^{90}_{pd} = \cos\left(2\pi\nu_b t + 2\varphi_2 - 2\varphi_1 - \varphi_3\right) + \cos\left(2\pi\nu_b t + 2\varphi_2 - \varphi_1 - 2\varphi_3\right) \text{ and} \tag{12}$$

$$I^{90}_{apd} = \cos\left(2\pi\nu_{13} t + \varphi_3 - \varphi_1\right), \tag{13}$$

are detected, where ν_{13} is the frequency between the two outer modes. If we assume $\varphi_1 = \varphi_3 = \varphi_{13}$, then Eqs. 12 and 13 become

$$I^{90}_{pd} = \cos\left(2\pi\nu_b t + 2\varphi_2 - 3\varphi_{13}\right) \text{ and} \tag{14}$$

$$I^{90}_{apd} = \cos\left(2\pi\nu_{13} t\right). \tag{15}$$

Additionally, we assume the mixed interference modes, $M_{1,m}$ with M_3 and $M_{3,m}$ with M_1 are much lower in signal power than the interference between M_1 and M_3, and are negligible. Once again, PD detects the mixed modal frequency, whereas the APD detects only the difference frequency between the two outer modes.

With the polarizer at 45°, all six modes interfere to produce numerous interference signals. The detected interference signals are

$$I^{45}_{pd} = \cos\left(2\pi\nu_b t + 2\varphi_2 - 3\varphi_{13}\right) + \cos\left(2\pi\nu_b + 3\varphi_2 - 2\varphi_{13}\right) \text{ and} \tag{16}$$

$$I^{45}_{apd} = \cos\left(2\pi\nu_{12} t + \varphi_2 - \varphi_{13}\right) + \cos\left(2\pi\nu_{23} t + \varphi_{13} - \varphi_2\right) + \cos\left(2\pi\nu_{13} t\right) \tag{17}$$

where ν_{12} is $\nu_2 - \nu_1$ and ν_{23} is $\nu_3 - \nu_2$. Once again, we assume the high frequency mixed interference modes are negligible in signal strength compared to the main modal beat frequencies ν_{12}, ν_{23}, and ν_{13}. The APD does detect the secondary beat frequency while the PD does not at this polarizer angle.

If the APD signal is examined first, ν_{12} differs slightly from ν_{23} (Fig. 1) due to frequency pulling effects [14]. However, both optical signals are detected, which means there are corresponding electrical signals, which get mixed in the transimpedance amplifier. Once the signals are bandpass filtered and amplified, the frequency difference between them can then be detected; this is the true secondary beat signal ν_b.

The signal from the PD is the sum of I^0_{pd} and I^{90}_{pd}, which produces no signal. This means the mixed modal frequency from I^0_{pd} and the secondary beat frequency from I^{90}_{pd} must be 180° out

#121356 - $15.00 USD Received 11 Dec 2009; revised 7 Jan 2010; accepted 11 Jan 2010; published 12 Jan 2010

of phase, causing destructive interference. Since we already assume $\varphi_1 = \varphi_3 = \varphi_{13}$, then this only occurs if $\varphi_2 + \varphi_{13} = 180^\circ$.

The optical schematic in Fig. 4 was used to verify this claim. In this schematic, the signal from the laser is split equally and two separate Glan-Thompson polarizers are aligned to the central and outer modes, respectively. This was confirmed using the optical spectrum analyzer. While the laser is in three mode operation, the signals from PD_0 and PD_{90} are indeed 180° out of phase, which can be seen in Fig. 5. To ensure this was not an anomaly with the laser, a different three mode laser (Model 098-2, JDSU) was used in the same setup. When this laser was in three mode operation, the same 180° difference was observed between PD_0 and PD_{90}, which can also be see in Fig. 5.

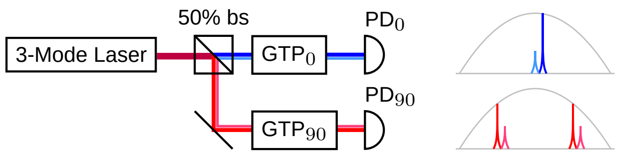

Fig. 4. (Color Online) Optical schematic for verifying the phase between I^0_{pd} and I^{90}_{pd}. Two Glan-Thompson polarizers (GTP) were used to isolate the inner and outer modes, which was verified using an optical spectrum analyzer.

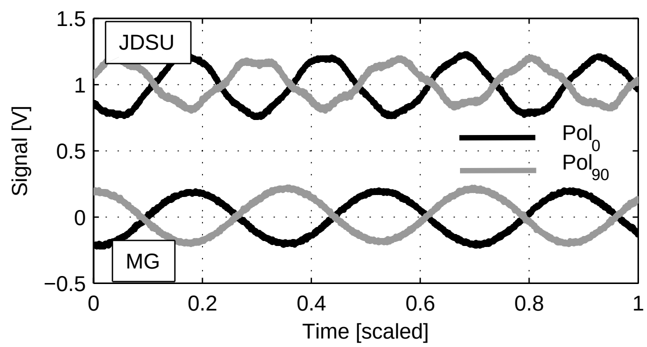

Fig. 5. Comparison of I^0_{pd} and I^{90}_{pd} for two different three mode lasers. The mixed modal beat frequencies are 180° out of phase which shows a low speed detector cannot detect the secondary beat frequency.

The mixed modal signal from the center mode, I^0_{pd}, was used to stabilize the three mode laser. The length of the laser tube, and thus frequency, was controlled via a thermo-electric cooler (TEC) which was driven by frequency fluctuations in I^0_{pd}. Using this signal and a TEC, the laser frequency from ν_2 was stabilized to better than 5.2×10^{-10}, when compared to an iodine stabilized laser. The Allan variance of the center mode fractional frequency stability is shown in Fig. 6(a).

The fractional noise density, shown in Fig. 6(b), had one minor peak at 10^{-2} Hz which is likely the time constant of the thermal mass in the system. A larger than desired thermal mass was used to buffer the laser from external disturbances which also limited the locking point stability due to long term environmental changes. The long term stability (months+) was not assessed due to this effect and the limited availability of the reference laser. Replacing the TEC-based actuator with a non-thermal method of controlling the cavity length would remove the unwanted thermal effects in the system and increase the locking point stability. A possible

#121356 - $15.00 USD Received 11 Dec 2009; revised 7 Jan 2010; accepted 11 Jan 2010; published 12 Jan 2010

solution is to use a sealed cavity laser with anti-reflectance coatings on one side of the laser tube and an externally located, piezo controlled laser mirror. A piezo-controlled mirror would increase bandwidth and remove most heat generation but alignment and the overall system concept need to be considered.

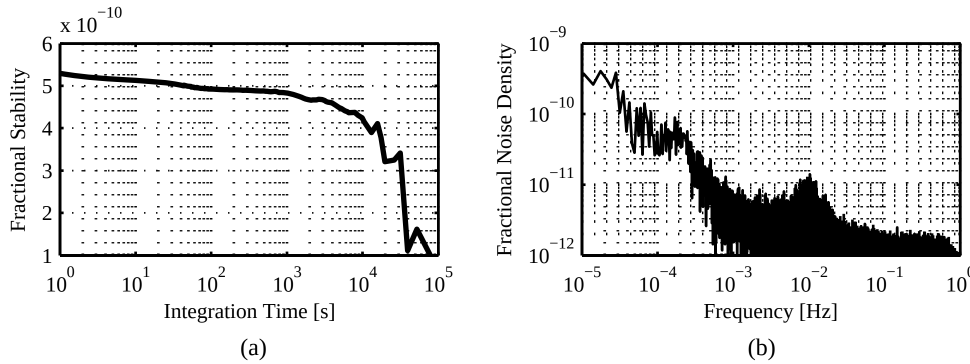

Fig. 6. Fractional frequency stability (a) and fractional noise density (b) of the center mode, ν_2, when compared with an Iodine stabilized laser using the signal generated from I_{pd}^{0}.

5. Conclusions

This research shows there is a detectable, intrinsic signal in a three mode HeNe gas laser which can be used for feedback stabilization. This mixed mode signal is different from the secondary beat frequency because direct measurement of the intermode frequencies is unnecessary. Additionally, the outer and outer-mixed mode signals are 180° from the central and central-mixed mode signal, causing destructive interference for detecting the secondary beat frequency.

This research sheds new light on secondary frequency standards with higher output power and better frequency stability. Future research into these mixed mode signals and stabilization may produce better practical standards at more wavelengths.

Acknowledgements

This work was supported by the Netherlands IOP under projects IPT06104 and IPT04001. The authors are grateful for many fruitful discussions with Dirk Voigt and the VSL Dutch Metrology Institute, as well as allowing us to use their Iodine stabilized reference laser. The authors would also like acknowledge Agilent Technologies for their equipment donation, parts of which were used in these experimental setups.

#121356 - $15.00 USD Received 11 Dec 2009; revised 7 Jan 2010; accepted 11 Jan 2010; published 12 Jan 2010